Nuclear Instruments and Methods in Physics Research B 376 (2016) 91–96

Contents lists available at ScienceDirect

Nuclear Instruments and Methods in Physics Research B

journal homepage: www.elsevier.com/locate/nimb

Laser ion beam production at CERN-ISOLDE: New features – More possibilities

S. Rothe [a,*], T. Day Goodacre [a,b], D.V. Fedorov [c], V.N. Fedosseev [a], B.A. Marsh [a], P.L. Molkanov [c], R.E. Rossel [a,d,e], M.D. Seliverstov [c], M. Veinhard [a], K.D.A. Wendt [d]

[a] CERN, Geneva, Switzerland
[b] School of Physics and Astronomy, The University of Manchester, Manchester, United Kingdom
[c] PNPI NRC KI, Gatchina, Russia
[d] Institut für Physik, Johannes Gutenberg-Universität, Mainz, Germany
[e] Faculty of Design, Computer Science and Media, Hochschule RheinMain, Wiesbaden, Germany

ARTICLE INFO

Article history:
Received 1 September 2015
Received in revised form 25 January 2016
Accepted 9 February 2016
Available online 26 March 2016

Keywords:
RILIS
Resonance laser ionization
ISOLDE

ABSTRACT

This article summarizes the current specifications and the latest features of the CERN-ISOLDE resonance ionization laser ion source (RILIS). This includes a description of the optical layout and the newly designed reference system. The ionization schemes for the laser ionized beams at ISOLDE are tabulated, including six new elements. All RILIS schemes are also made publicly available in the RILIS elements on-line database. Finally, we announce a paradigm shift in RILIS operation – the combination of a machine protection and a monitoring and control system has enabled on-call operation of the laser ion source for selected beams in 2014 and has become the standard mode of operation in 2015.

1. Introduction

The resonance ionization laser ion source (RILIS) [1,2] is the most frequently applied ion source type of the CERN-ISOLDE radioactive ion beam facility [3]. The method of step-wise resonant laser excitation and ionization of the products from the nuclear reactions inside the ISOLDE target is both highly selective and efficient. To keep up with the increase in demand, the RILIS laser installation is continuously being upgraded and improved [4–6]. Between the end of 2012 and the beginning of 2014, operation of ISOLDE was interrupted for a scheduled long shutdown of the CERN accelerator complex (LS1) for the upgrade and maintenance of e.g. the Large Hadron Collider (LHC). During this period a number of major RILIS upgrades could be implemented. The RILIS room was extended and the laser reference area and launch point to the GPS target underwent a reconstruction. The RILIS machine protection system (RMPS) was implemented in conjunction with a refined remote control and monitoring system which enabled the first RILIS on-call operation for selected runs during the 2014 ISOLDE on-line period. In addition to these immediate upgrades, studies were ongoing to increase availability, efficiency and selectivity of RILIS beams; ionization schemes for additional elements were developed and existing schemes have been improved. Laser ionization to the 2^+ state has been applied for barium [7] and mercury was ionized inside the FEBIAD-type ion source cavity [8]. The time-of-flight laser ion source (ToF-LIS) project [9], which combines high resistance cavities with laser-synchronized microsecond beam-gating, has been continued. In this paper we present the current status of the RILIS and highlight the new features and ongoing developments.

2. The RILIS laser system

Ion beams of more than 35 chemical elements have been produced using the ISOLDE-RILIS. Each ionization scheme requires a specific laser configuration, typically involving the simultaneous use of up to three of the tunable lasers. To provide access to the wavelengths required for the different excitation and ionization schemes, the RILIS laser system is composed of six broadly tunable lasers, operating in the visible to near infra-red wavelength range. The laser parameters (summarized in Table 1) are optimized for the hot cavity ionization environment such that the 10 kHz pulse repetition rate matches the mean residence time (100 μs) of the atoms in the 34 mm long hot cavity and the 5–20 GHz line-width of the tunable lasers comfortably exceeds the Doppler broadening of the optical transitions at the operating temperature of ~2000 °C.

* Corresponding author.
E-mail address: sebastian.rothe@cern.ch (S. Rothe).

http://dx.doi.org/10.1016/j.nimb.2016.02.024
0168-583X/

Table 1
Overview of the key parameters of laser sources available at RILIS.

Laser	Function	Wavelength	Power, max.	Pulse width
Nd:YAG	Dye pumping	532 nm	100 W	8 ns
Edgewave CX16III-OE	Dye pumping	355 nm	20 W	11 ns
Nd:YAG	Ti:Sa pumping	532 nm	60 W	170 ns
Photonics Industries DM-60–532			$M^2 < 30$	
Nd:YVO_4	Non-resonant ionization/	532 nm	40 W	17 ns
Coherent Blaze 532–40-HE	Ti:Sa and dye pumping		$M^2 < 1.3$	
Dye laser	Resonance atomic excitation,	390–860 nm	20 W (fundamental)	7 ns
Sirah Credo	Spectroscopy	270–390 nm	2.5 W SHG	6 ns
	9 GHz linewidth	210–270 nm	0.2 W THG	5 ns
(NB-)Dye laser	Resonance atomic excitation,	390–860 nm	10 W (fundamental)	10 ns
DMK MSS	(NB) spectroscopy	270–390 nm	1 W SHG	
	15 GHz (0.8 GHz)	210–270 nm	0.2 W THG	
(NB-)Ti:Sa laser	Resonance atomic excitation,	680–950 nm	6 W (fundamental)	30–50 ns
CERN/Mainz	(NB) spectroscopy	340–475 nm	1 W SHG	
	5 GHz (0.8 GHz)	210–315 nm	0.15 W THG,FHG	

2.1. Optical layout

The optical layout of the RILIS is illustrated in Fig. 1. The three RILIS dye lasers (2× *Sirah Credo*, 1× *MSS*) are pumped by a single diode-pumped solid-state (DPSS) frequency doubled Nd:YAG laser (*Edgewave GmbH*). The pump light emerging from each of the two 532 nm output ports of the *Edgewave* pump laser is typically directed to the two *Credo* dye lasers. The power distribution between the output ports is adjusted by fine-tuning of the temperature-controlled phase matching of the internal harmonic generation units. A third output port may be used to extract up to 20 W of 355 nm third harmonic light for UV pumping of one dye laser, extending the fundamental tuning range down to 390 nm. Adjustable beam expanders (*Edmund Optics*) are used to match the pump beam to the requirements of the tunable lasers.

The three RILIS titanium:sapphire (Ti:Sa) lasers [5,10] are pumped by DPSS Nd:YAG lasers (2× *DM-60–532, Photonics Industries, Inc.*). A pump beam distribution system consisting of beam expanders (factor of 3 expansion), half-wave plates ($\lambda/2$) and high-power polarizing beam splitter (PBS) cubes (*Edmund Optics*) allows for variable pump power distribution, thus adjusting the gain of each Ti:Sa laser individually.

One additional *Photonics* and one additional *Edgewave* laser is available on-site, serving as spares, minimizing downtime in the event of a pump laser failure. Frequency conversion using single-pass frequency mixing in BBO or BiBO crystals is applied to extend the available wavelength spectrum. Up to third and fourth harmonics (THG, FHG) are generated from the fundamental output of the dye and Ti:Sa lasers respectively, using the frequency conversion unit (FCU). The wavelengths of the tunable lasers are measured using fiber-coupled wavelength meters *Angstrom HighFinesse WS6*, *WS7* and a *Cluster LM007*.

When required, a dedicated frequency-doubled DPSS Nd:YVO_4 laser (*Lumera* (now *Coherent*) *Blaze*) provides the radiation (40 W output power at 532 nm) for non-resonant ionization of highly excited atoms. The favorable TEM_{00} beam profile and low M^2 enable good focusing of the beam, and therefore better power transmission, into the ion source. The added low jitter option for the external TTL trigger allows synchronization of the *Blaze* pulse with a precision of 3 ns. Our measurements indicate that the use of the *Blaze* laser has increased the efficiency of schemes using a non-resonant final step by up to a factor of two with respect to the previously used *Edgewave* laser. In addition, the laser has been demonstrated to be capable of simultaneously pumping of up to two dye lasers with high efficiency [11].

For focusing the laser beams into the ion source cavity, located at a distance of ~20 m from the laser table, several telescope configurations are used: adjustable beam expanders (*Edmund Optics*) or spherical lens telescopes mounted on optical rails for circular or near-circular laser beams. Cylindrical lens telescopes are used for elliptical beams with an aspect ratio exceeding 2:1, such as the UV beams typically obtained after frequency conversion processes. After the telescopes the beams are directed to one of the two launch points where they exit the laser room to be transported via fixed optics inside the separator area through the magnet window, to converge towards the 3 mm aperture of the hot cavity ion source at one of the two ISOLDE frontends named HRS or GPS (corresponding to the High Resolution Separator or General Purpose Separator to which they are connected [3]).

2.2. Laser pulse synchronization

The TTL trigger signals for each of the four pump lasers are generated by a multi-output master clock and delay generator (*Quantum Composers 9538*). Adjusting the delay with respect to the master trigger signal (T0) enables synchronization of the laser pulses. Since a single pump laser typically pumps multiple dye-lasers, pulse synchronization is achieved through the use of optical delay lines. When pumping multiple Ti:Sa lasers from a single source, synchronization is achieved by fine-tuning the resonator gain by adjusting the pump power or focusing. The T0 signal is distributed throughout the RILIS and the ISOLDE patch panels using an optocoupler-isolated 12× TTL fanout (*Meinberg SDU-OC-TTL*). This facilitates the synchronization of the experimental setups of the ISOLDE users with the RILIS pulse timing.

2.3. Improved in-source laser spectroscopy

For special applications e.g. for high-resolution in-source laser spectroscopy studies of atomic transitions, or isomer separation through the selective excitation of atomic hyperfine-structure components [12] the *MSS* dye laser and the Ti:Sa lasers can be switched to a reduced linewidth or narrow bandwidth (NB) mode. The NB–Ti:Sa [10,13] was used successfully for in-source laser spectroscopy campaigns of polonium, astatine, gold and mercury isotopes [14,15,8], scheduled in 2014 and 2015. During these

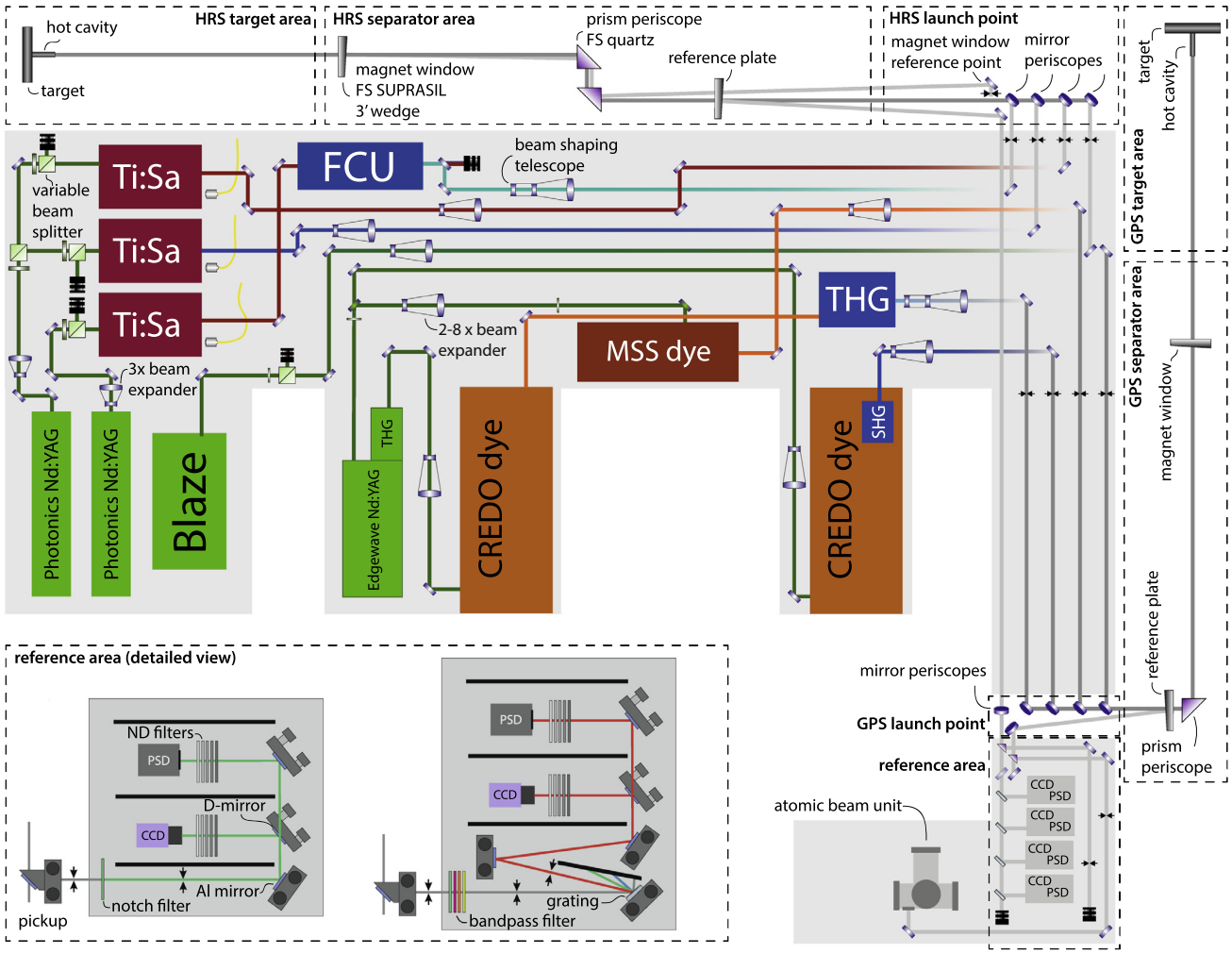

Fig. 1. The detailed optical layout of the RILIS (not to scale). Further explanations are given in the text.

campaigns the refined LabVIEW based RILIS data acquisition system [10,16,17] was used to coordinate the NB–Ti:Sa scans with the different detection setups (Leuven Windmill [18] and ISOLTRAP MR-ToF MS [19]) and the Proton Synchrotron Booster pulse supercycle in addition to recording and visualizing the spectroscopy data and relevant auxiliary parameters.

3. Laser launch points and separator areas

Outside of the laser laboratory, access to the optical path is strictly forbidden while the proton beam hits the target and highly restricted during the ISOLDE on-line period, due to radiological protection measures. To maintain compatibility to all ionization schemes broadband UV-grade fused-silica (FS) optics (transport prisms, windows and beam samplers) are used in the areas with limited access.

The transport of the laser beams to the HRS separator is particularly challenging. The long distance of 23 m combined with the temperature difference between the RILIS laboratory and the separator zone results in fluctuations in the laser beam position. The HRS launch area was therefore reconfigured and optimized first [10] where beam transport losses were reduced through the use of dielectric coated mirrors as a replacement for the previously used uncoated prism periscopes and horizontal and vertical controls have been disentangled using a layout adapted to the angle of 58° under which the lasers are directed to the HRS separator area. The new system allows up to four laser beams to be launched towards the HRS. One of them can be sent via a separate optical path through the second HRS magnet into the gas-filled RFQ ion cooler-buncher (ISCOOL) where it can be used for optical pumping [20] or for other spectroscopic applications. The magnet window of the first HRS magnet has been placed onto a 70 cm long extension pipe equipped with a port aligner (*Lesker PA35-T*), which enables direct access from outside the magnet. The 1.5 inch diameter window (*Corning 7980, grade 0C supplied by Island Optics Ltd.*, 3 arcmin wedge) is mounted in an off-the-shelf CF flange (*Thorlabs VPCH2-FL*). A *Viton* seal is used instead of the copper gasket to allow for fast interventions. Using the port aligner, the surface reflections of the window can be directed to the RILIS room where they serve as an additional ion source reference point and can be used to assess the cleanliness or performance of the window itself or optics downstream of the primary reference plate. Using these reference beams we have observed thermal lensing effects, when sending the 40 W *Blaze* laser beam to the HRS. These were attributed to be caused by the dust on the reflective surface of the prisms. We therefore have designed a prism mount (available from *Liop-TEC GmbH*) that creates a sealed air gap for this sensitive surface. To assess the transport efficiency of the lasers to the ion source, an ISOLDE target unit was equipped with a laser powermeter sensor (*Gentec UP19K-15S-H5-D0*) and a shortened tungsten ionizer cavity (20 mm length). The powermeter sensor was calibrated at the ISOLDE Off-line laboratory [21]. The sensor read-out at ISOLDE is conveniently available through the existing thermocouple infrastructure.

Table 2
Currently available excitation and ionization schemes at ISOLDE RILIS, updated from [4,6]. The recently developed or newly applied schemes are highlighted in bold. Schemes that were newly developed, improved or where new data is available carry a reference where further details can be found. Laser dyes are abbreviated as follows: Pyr. – Pyridine, Rh. – Rhodamine, Fl. – Fluorescein, DCM – 4-(dicyanomethylene)-2-methyl-6-(4-dimethylaminostyryl)-4H-pyran, Ph. – Phenoxazone, Styr. – Styryl, Pyrr. – Pyrromethene, Cou. – Coumarin.

Element	λ_1, vac (nm)	Laser	λ_2, vac (nm)	Laser	λ_3, vac (nm)	Laser	Notes, Refs.
$_{3}$Li	670.96	Ph.9	610.53	DCM	532	Nd:YVO_4	[7]
$_{4}$Be	234.93	Pyr.1, THG Ti:Sa, THG	297.41	Rh.B, SHG	–		
$_{12}$Mg	285.30	Rh.6G, SHG Ti:Sa, THG	552.99	Fl.27	532	Nd:YVO_4	
$_{13}$Al	308.30 309.37	Rh.B, SHG Rh.B, SHG	532	Nd:YVO_4	–		
$_{20}$Ca	422.79 272.25	Ti:Sa, SHG Fl.27, SHG	585.91 532	Rh.B Nd:YVO_4	654.12 –	DCM	[26,27]
$_{21}$Sc	327.46	Ph.9, SHG	720.03	Pyr.2	532	Nd:YVO_4	
$_{24}$Cr	357.97	Ti:Sa, SHG Pyr.2, SHG	698.03	Pyr.1 Ti:Sa	579.31	Rh.6G	[28] [28]
$_{25}$Mn	279.91	Rh.6G, SHG Ti:Sa, THG	628.44	DCM	647.52	DCM	
$_{27}$Co	304.49	Rh.B, SHG	544.61	Fl.27	532	Nd:YVO_4	
$_{28}$Ni	305.17	Rh.B, SHG	611.28	Rh.B	748.42	Ti:Sa Styr.8	[10]
$_{29}$Cu	327.49	Ph.9, SHG	287.98	Rh.6G, SHG	–		
$_{30}$Zn	213.92	Ph.9, THG Ti:Sa, FHG	636.41	DCM	532	Nd:YVO_4	
$_{31}$Ga	287.51 294.50	Rh.6G, SHG Ti:Sa, THG	532	Nd:YVO_4	–		
$_{32}$Ge	275.54	Fl.27, SHG	569.35	Rh.6G	532	Nd:YVO_4	[29]
$_{39}$Y	414.28	Styr.9, SHG	662.55	Ph.9	532	Nd:YVO_4	
$_{47}$Ag	328.16	Ph.9, SHG	546.70 421.21	Fl.27 Ti:Sa, SHG	532	Nd:YVO_4	[10]
$_{48}$Cd	228.87	Pyr.1, THG Ti:Sa, FHG	644.02	DCM	532	Nd:YVO_4	[10]
$_{49}$In	304.02 325.70	Rh.B, SHG Ti:Sa, THG Ph.9, SHG	532	Nd:YVO_4	–		
$_{50}$Sn	286.30	Rh.6G, SHG	811.40	Styr.9	823.68	Styr.9	
$_{51}$Sb	217.65	Ph.9, THG	560.36	Rh.6G	532	Nd:YVO_4	
$_{52}$Te	214.35	Ti:Sa, FHG	573.52	Rh.6G	901.51	Ti:Sa	[29]
$_{56}$Ba	350.21	Pyr.1, SHG Ti:Sa, SHG	627.86	DCM	–		[7]
$_{56}$Ba^{2+}	455.53	Ti:Sa, SHG	223.35	Ti:Sa, FHG	532	Nd:YVO_4	[7]
$_{59}$Pr	461.90	Ti:Sa, SHG	900.00	Ti:Sa	532	Nd:YVO_4	[10]
$_{60}$Nd	588.95	Rh.6G	597.10	Rh.B	597.10	Rh.B	
$_{62}$Sm	600.58	Rh.B	675.34	Ph.9	676.37	Ph.9	
$_{65}$Tb	579.72	Rh.6G	551.80	Fl.27	618.43	Rh.B	
$_{66}$Dy	626.08	DCM	607.67	Rh.B	532	Nd:YVO_4	
$_{67}$Ho	405.50	Ti:Sa, SHG	623.43	DCM	532 811.00	Nd:YVO_4 Ti:Sa, AIS	

Table 2 (*continued*)

Element	λ_1, vac (nm)	Laser	λ_2, vac (nm)	Laser	λ_3, vac (nm)	Laser	Notes, Refs.
$_{70}$Yb	267.28 555.80	Ti:Sa, THG Pyrr.567	523 581.23	Nd:YVO_4 Rh.6G	 581.23	 Rh.6G	[10]
$_{79}$Au	267.67	Cou.540A, SHG Ti:Sa, THG	306.63	DCM, SHG	674.08	Ph.9	
$_{80}$Hg	253.73	Ti:Sa, THG Styr.8, SHG	313.28	DCM, SHG	532	ND:YVO4	
$_{81}$Tl	276.87	Rh.110, SHG Ti:Sa, THG	532	Nd:YVO_4	–		
$_{82}$Pb	283.39	Rh.6G, SHG	600.36	Rh.B	532	Nd:YVO_4	
$_{83}$Bi	306.86	Rh.B, SHG	555.36	Fl.27	532	Nd:YVO_4	
$_{84}$Po	255.88	Ti:Sa, THG Styr.8, THG	843.62	Ti:Sa Styr.9	532 593.93	Nd:YVO_4 Rh.6G, Ryd.	[26] [26]
$_{85}$At	216.29	Ti:Sa, FHG	795.45 915.46	Ti:Sa Ti:Sa	620.54 532	DCM, Ryd. Nd:YVO_4	[30] [10]

An extension of the RILIS room by 6 m^2 has liberated space for an improved area for launching the beams to the GPS target and for the construction of an extended laser beam reference and monitoring area equipped with a compact thermal atomic beam unit. The GPS launch point was upgraded the same way as the HRS: the uncoated prisms were replaced by dielectric mirrors and four independent optical beam paths are now available.

4. Laser observation system

The global layout of the re-configured reference area is illustrated in Fig. 1. Two example configurations of the four available observation sites, are illustrated in the inset.

The reference plates for HRS and GPS, located half-way between the launch points and the ion sources, are wedged and therefore create two reference beams separated by ~15 mm when reaching the reference area. One of the beams is picked off using a prism and directed to the absolute reference point set by an adjustable iris separately for HRS and GPS. A powermeter positioned after the iris enables relative measurements of the power in the ion source. The other reference beam is sent to the newly designed observation system comprising a row of four wedged pick-up plates sampling the reference beam, thus creating several reference beamlets which passing via optical filters, D-shaped mirrors and diffraction gratings enable separate imaging of the laser beams with different wavelengths by dedicated CCD cameras and position sensitive detectors (PSDs). Each PSD is a segmented photodiode which is linked to a piezo actuated active feedback stabilization system (*MRC Systems*). The use of absorptive color glass bandpass, dielectric neutral density or low-pass filters prevents stray light from reaching the sensors. An additional laser table is dedicated to accommodate an atomic beam unit (based on [22]), which is to be used as a reference for in-source laser spectroscopy and for off-line ionization scheme developments using the RILIS lasers.

5. Remote control, monitoring and on-call operation

Essential parameters (wavelengths, laser power, ion beam current, proton beam information etc.) are accessible to a LabVIEW-based RILIS remote monitoring and control system (known as REACT) which is under continual development [16]. The laser operating parameters are visible publicly via a RILIS status viewer website [23]. The REACT also allows remote control of laser parameters and has recently been used to develop feedback stabilization of laser wavelength, output power, and timing [24]. These tools liberate the RILIS operator from the need to perform repetitive tasks and instead focus on developing the RILIS.

This is supplemented by an autonomous and robust FPGA-based (*National Instruments CompactRIO*) RILIS Machine Protection System which has been developed to detect, and instantly act upon, a hazardous laser malfunction such as a dye flow fault or a dye leak. The system is capable of sending status information, warnings and errors via SMS to the operator in charge.

These innovations (REACT & RMPS), coupled with the use of inherently reliable industrial-grade laser equipment, enable round-the-clock RILIS operation, with up to 3000 h of annual running time for physics experiments. The combination of REACT and RMPS has enabled the first on-call RILIS operation for selected runs in 2014. This practice was successful and has become the standard mode of RILIS operation in 2015. It should be noted, however, that the preparation for reliable on-call operation comes at the cost of increased complexity, required precision and therefore man-hour requirements during setup. The implication of this is that, for a given ionization scheme, the time required for laser setup can be up to 50% longer. Fortunately this can be compensated for by the reduced man-power requirement of normal operation and the flexibility of the dual RILIS system which, to some extent, enables concurrent laser operation and setup.

6. New ionization schemes and the RILIS elements database

Ionization schemes are the backbone of the RILIS operation. Since the integration of the solid-state Ti:Sa lasers to the RILIS laser system, creating the Dual RILIS, and therefore extending the accessible wavelength range further into to the infra-red and blue spectrum, the choice of ionization paths has become more flexible. Since our previous report [6] six additional schemes have been developed or were applied on-line for the first time at ISOLDE and are therefore available to the users of the facility. Table 2 gives an overview of the ionization schemes that have been applied for ion beams extracted using ISOLDE-RILIS.

The RILIS ionization schemes are also made available in the public RILIS scheme database (RILISDB) [25]. The database features visualization of the ionization schemes (colors and transition strengths), all information may be referenced. The information can be edited and new schemes can be added by registered users.

7. Ion source developments

The increased availability of the ISOLDE off-line separator during LS1 has enabled us to pursue long standing ion source development objectives. This includes the continuation of the ToF-LIS project for improved RILIS selectivity [31]. ToF-LIS aims to combine a reduction in the laser ion bunch width (through the use of high resistance cavities and an additional field-free region for time-focussing) with a microsecond ion beam gate, thus suppressing the DC surface ion background. The selectivity improvement is set by the duty factor of the beam gate. A 10 μs wide beam gate was set to transmit laser ionized gallium ions and allowed for a suppression of ^{39}K by one order of magnitude. More details can be found in [9].

Laser ionization inside the FEBIAD type VADIS ion source has been investigated at the off-line separator laboratory and was first employed on-line for the in-source laser spectroscopy of neutron-rich mercury isotopes, produced in a liquid lead target, coupled to a VADIS ion source. In off-line tests with Ga and on-line tests with radiogenic Hg and Cd isotopes the laser ionization observed at low anode voltages was shown to be not less efficient than typical VADIS electron impact ionization. More details can be found in [8].

Acknowledgements

This project has received funding through the European Unions Seventh Framework Programme for Research and Technological Development under Grant Agreements 262010 (ENSAR), 267194 (COFUND), and 289191 (LA^{3}NET).

References

[1] V. Mishin, V. Fedoseyev, H.-J. Kluge, et al., Chemically selective laser ion-source for the CERN-ISOLDE on-line mass separator facility, Nucl. Instr. Meth. B 73 (4) (1993) 550–560, http://dx.doi.org/10.1016/0168-583x(93)95839-w.
[2] V. Fedoseyev, G. Huber, U. Köster, et al., The ISOLDE laser ion source for exotic nuclei, Hyperfine Interact. 127 (1/4) (2000) 409–416, http://dx.doi.org/10.1023/a:1012609515865.
[3] E. Kugler, The ISOLDE facility, Hyperfine Interact. 129 (1/4) (2000) 23–42, http://dx.doi.org/10.1023/a:1012603025802.
[4] V. Fedosseev, L.-E. Berg, N. Lebas, et al., ISOLDE RILIS: new beams new facilities, Nucl. Instr. Meth. B 266 (19–20) (2008) 4378–4382, http://dx.doi.org/10.1016/j.nimb.2008.05.038.
[5] S. Rothe, B.A. Marsh, C. Mattolat, et al., A complementary laser system for ISOLDE RILIS, J. Phys. Conf. Ser. 312 (5) (2011) 052020, http://dx.doi.org/10.1088/1742-6596/312/5/052020.
[6] V.N. Fedosseev, L.-E. Berg, D.V. Fedorov, et al., Upgrade of the resonance ionization laser ion source at ISOLDE on-line isotope separation facility: New lasers and new ion beams, Rev. Sci. Instr. 83 (2) (2012) 02A903, http://dx.doi.org/10.1063/1.3662206.
[7] T. Day Goodacre, et al., Laser ionized ion beams of Li^+, Ba^+ and Ba^{++} using the ISOLDE-RILIS (unpublished results).
[8] T. Day Goodacre, et al., Blurring the boundaries between ion sources: The application of the RILIS inside a FEBIAD type ion source at ISOLDE, Nucl. Instr. Meth. B 376 (2016) 39–45.
[9] S. Rothe, et al., Advances in surface ion suppression from RILIS: towards the Time-of-Flight laser ion source (ToF-LIS), Nucl. Instr. Meth. B 376 (2016) 86–90.
[10] S. Rothe, An all-solid state laser system for the laser ion source RILIS and in-source laser spectroscopy of astatine at ISOLDE/CERN (Ph.D. thesis), Mainz U., presented 24 Sep 2012 (2012). http://dx.doi.org/10.17181/CERN.0HNZ.7Z6X.
[11] B. Marsh, V. Fedosseev, D. Fink, et al., Suitability test of a high beam quality Nd:YVO4 industrial laser for the ISOLDE RILIS installation., Tech. Rep. CERN-ATS-Note-2013-007 TECH (Jan 2013). http://dx.doi.org/10.17181/CERN.F65D.P3NR.
[12] B. Marsh, B. Andel, A. Andreyev, et al., New developments of the in-source spectroscopy method at RILIS/ISOLDE, Nucl. Instr. Meth. B 317 (2013) 550–556, http://dx.doi.org/10.1016/j.nimb.2013.07.070.
[13] S. Rothe, V. Fedosseev, T. Kron, et al., Narrow linewidth operation of the RILIS titanium: sapphire laser at ISOLDE/CERN, Nucl. Instr. Meth. B 317 Part B (2013) 561–564, http://dx.doi.org/10.1016/j.nimb.2013.08.058.
[14] D.A. Fink, T.E. Cocolios, A.N. Andreyev, et al., In-source laser spectroscopy with the laser ion source and trap: first direct study of the ground-state properties of Po 217 219, Phys. Rev. X 5 (1). http://dx.doi.org/10.1103/physrevx.5.011018.
[15] L.P. Gaffney, T. Day Goodacre, A. Andrei, et al., In-source laser spectroscopy of mercury isotopes, Tech. Rep. CERN-INTC-2014-060. INTC-P-424, CERN, Geneva (Oct 2014). URL: https://cds.cern.ch/record/1953719.
[16] R. Rossel, V. Fedosseev, B. Marsh, et al., Data acquisition remote control and equipment monitoring for ISOLDE RILIS, Nucl. Instr. Meth. B 317 (2013) 557–560, http://dx.doi.org/10.1016/j.nimb.2013.05.048.
[17] R.E. Rossel, Network distributed data acquisition, storage, and graphical live display software for a laser ion source at CERN, Tech. Rep. CERN-OPEN-2015-005, CERN, Geneva (Aug 2014). http://dx.doi.org/10.17181/CERN.LYUP.S9AN.
[18] A.N. Andreyev, J. Elseviers, M. Huyse, et al., New type of asymmetric fission in proton-rich nuclei, Phys. Rev. Lett. 105 (2010) 252502, http://dx.doi.org/10.1103/PhysRevLett. 105.252502.
[19] R. Wolf, D. Beck, K. Blaum, et al., On-line separation of short-lived nuclei by a multi-reflection time-of-flight device, Nucl. Instr. Meth. A 686 (2012) 82–90, http://dx.doi.org/10.1016/j.nima.2012.05.067.
[20] B. Cheal, J. Billowes, M.L. Bissell, et al., Collinear laser spectroscopy of manganese isotopes using optical pumping in ISCOOL., Tech. Rep. CERN-INTC-2010-073. INTC-P-286, CERN, Geneva (Oct 2010). URL: https://cds.cern.ch/record/1298606.
[21] A. Zadvornaya, et al., Development of a power meter equipped target for ISOLDE RILIS, Tech. Rep. CERN-STUDENTS-Note-2013-247 (Oct 2013). URL: https://cds.cern.ch/record/1618369.
[22] T. Kron, R. Ferrer-Garcia, N. Lecesne, V. Sonnenschein, S. Raeder, J. Rossnagel, K. Wendt, Control of RILIS lasers at IGISOL facilities using a compact atomic beam reference cell, Hyperfine Interact. 216 (1) (2013) 53–58, http://dx.doi.org/10.1007/s10751-012-0756-7.
[23] S. Rothe, R. Rossel, The Status of the RILIS lasers (2015) [cited 2015–8-30]. URL: http://cern.ch/rilis/status.
[24] R.E. Rossel, A distributed monitoring and control system for the laser ion source RILIS at CERN-ISOLDE (Master's thesis), Fachhochschule Wiesbaden, presented 29 Oct 2015 (Sep 2015). http://dx.doi.org/10.17181/CERN.L5N9.2GCS.
[25] S. Rothe, M. Klein, RILIS DB – an ionization scheme database for laser ion sources (2015) [cited 2015–8-30]. URL: http://cern.ch/riliselements.
[26] D.A. Fink, Improving the selectivity of the ISOLDE resonance ionization laser ion source and in-source laser spectroscopy of polonium (Ph.D. thesis), Heidelberg U., presented 23 Jan 2014 (2014). http://dx.doi.org/10.17181/CERN.R8QG.WACQ.
[27] B.A. Marsh, V.N. Fedosseev, D.A. Fink, et al., RILIS applications at CERN/ISOLDE, Hyperfine Interact. 227 (1–3) (2014) 101–111, http://dx.doi.org/10.1007/s10751-014-1051-6.
[28] T. Day Goodacre, K. Chrysalidis, D. Fedorov, et al., Identification of autoionizing states of atomic chromium for resonance photo-ionization at the ISOLDE-RILIS, ArXiv e-prints arXiv:1512.07875 [physics.atom-ph]. URL: https://arxiv.org/abs/1512.07875.
[29] T.D. Goodacre, D. Fedorov, V. Fedosseev, et al., Laser resonance ionization scheme development for tellurium and germanium at the dual Ti:Sa-Dye ISOLDE RILIS, Nucl. Instr. Meth. A (2016), http://dx.doi.org/10.1016/j.nima.2015.10.066.
[30] S. Rothe, A.N. Andreyev, S. Antalic, et al., Measurement of the first ionization potential of astatine by laser ionization spectroscopy, Nat. Commun. 4 (2013) 1835, http://dx.doi.org/10.1038/ncomms2819.
[31] V.I. Mishin, A.L. Malinovsky, D.V. Mishin, Resonant ionization laser ion source (RILIS) with improved selectivity achieved by ion pulse compression using in-source time-of-flight technique, AIP Conf. Proc. 1104 (1) (2009) 207–212, http://dx.doi.org/10.1063/1.3115604.